Published in final edited form as:
Science. 2010 February 19; 327(5968): 986–990. doi:10.1126/science.1182826.

Asymmetric Cooperative Catalysis of Strong Brønsted Acid-Promoted Reactions Using Chiral Ureas

Hao Xu, **Stephan J. Zuend**, **Matthew G. Woll**, **Ye Tao**, and **Eric N. Jacobsen***
Department of Chemistry and Chemical Biology, Harvard University, Cambridge, MA 02138, USA

Abstract

Cationic organic intermediates participate in a wide variety of useful synthetic transformations, but their high reactivity can render selectivity in competing pathways difficult to control. We describe a strategy for inducing enantioselectivity in reactions of protio-iminium ions, wherein a chiral catalyst interacts with the highly reactive intermediate through a network of non-covalent interactions. This leads to an attenuation of the reactivity of the iminium ion, and allows high enantioselectivity in cycloadditions with electron-rich alkenes (the Povarov reaction). A detailed experimental and computational analysis of this catalyst system has revealed the precise nature of the catalyst-substrate interactions and the likely basis for enantioinduction.

The proton (H^+) is the simplest—and arguably most versatile—catalyst for organic reactions, mediating an extraordinary range of biological and synthetic transformations (1). Although a proton cannot be rendered chiral, enantioselective Brønsted acid catalysis is attainable through the influence of the acid's conjugate base and through medium effects. The former strategy, involving use of chiral acids, has proven particularly useful as demonstrated in the design and application of chiral phosphoric acids (2,3,4), *N*-triflyl phosphoramides (5), aryl sulfonic acids (6), and Lewis acid- (7,8) or thiourea-assisted Brønsted acids (9,10). The use of medium effects has been less straightforward, and chiral solvents have been investigated in asymmetric catalysis with comparatively limited success (11). The recent discovery of anion-binding pathways (12,13) in reactions catalyzed by chiral small-molecule H-bond donor catalysts such as urea and thiourea derivatives (14) suggests an alternative strategy that combines elements of both approaches, wherein a chiral catalyst might associate with a protonated substrate through the counteranion, and induce enantioselectivity in additions to the cationic electrophile through specific secondary interactions with the charged species.

This idea was explored in the context of the formal [4+2] cycloaddition of *N*-aryl imines and electron-rich olefins, also known as the Povarov reaction. (15) This Brønsted-acid catalyzed reaction affords tetrahydroquinoline derivatives with concomitant generation of up to three contiguous stereogenic centers, and enantioselective Lewis acid or phosphoric acid-catalyzed variants have been identified recently (16,17,18). The acid-catalyzed Povarov reaction between benzylidene aniline **2a** and 2,3-dihydrofuran **3** was selected as a model reaction (Fig. 1A), and a broad range of chiral urea and thiourea derivatives developed and studied previously in our laboratory—as well several different Brønsted acids—were evaluated as catalysts for this transformation (Table S1,19). Using this approach, the combination of the bifunctional sulfinamido urea derivative **1a** (20) and *ortho*-nitrobenzenesulfonic acid (NBSA) was found to catalyze the model reaction with high enantioselectivity (Figs. 1B and 1C, entry 1). The importance of both the urea and

*To whom correspondence should be addressed. jacobsen@chemistry.harvard.edu.

sulfinamide groups in the catalyst became evident in structure-reactivity/enantioselectivity studies. Thiourea derivative **1b** is an efficient catalyst but induced lower enantio- and diastereoselectivity (entry 2), whereas the diastereoisomeric (*R*,*R*,*S*)-sulfinamido urea **1c** promoted a much slower and poorly selective reaction (entry 3). In addition, reactions catalyzed by phosphinic amide urea **1d** displayed a modest selectivity, and pivalamide urea **1e** and amino urea **1f** both induced low reactivity and selectivity (entries 4–6). These results suggest a cooperative role of the urea and sulfinamide groups of **1a** in the rate- and enantioselectivity determining steps of the catalytic reaction.

Under optimized conditions, the Povarov reaction catalyzed by **1a** was found to be applicable to different nucleophiles and a wide variety of *N*-aryl imines (Fig 2A–B). The highest enantioselectivities were observed in reactions carried out under cryogenic conditions, using a 2:1 ratio of **1a** to NBSA in order to ensure complete suppression of the racemic pathway catalyzed by NBSA alone. Lactam-substituted tetrahydroquinoline derivatives $\mathbf{6_{exo}}$ were obtained in high enantio- and diastereoselectivities by reaction of benzaldimines **2** with vinyllactam **5**. Tricyclic hexahydropyrrolo-[3,2-*c*]quinoline derivatives $\mathbf{8_{exo}}$ were generated in an analogous manner by cyclization of *N*-Cbz-protected 2,3-dihydropyrrole **7** with **2**. Although moderate diastereoselectivities favoring the *exo* diastereomer were obtained in this case ($\mathbf{8_{exo}/8_{endo}}$ =1.4–4.2: 1), this product was also generated in high enantiomeric excess (90–98% *ee*), and could be isolated in diastereomerically pure form in useful yields (45–73%). In general, imines derived from electron-deficient aldehydes—especially imines derived from glyoxylate esters—underwent reaction more rapidly in the Povarov reaction, but uniformly high enantioselectivities were obtained despite these reactivity differences.

Povarov reactions between glyoxylate imines **9a** or **9b** with 2,3-dihydropyrrole **7** provide the *endo* products in high enantioselectivity. This represents a direct route to the core tetrahydroquinoline structure of a variety of important, biologically active compounds (21,22,23), including martinelline (**11**,Fig. 2C), the first naturally occurring non-peptide natural product identified as a bradykinin B1 and B2 receptor antagonist (24). The enantioselective, catalytic Povarov method provides an efficient, enantioselective route to this natural product and its analogs (25), thereby solving a long-standing synthetic challenge.

The cooperative activity of an acid and a chiral organic molecule may represent a general strategy for asymmetric catalysis (9,10), and we thus undertook a detailed experimental and computational study to elucidate the mechanism of catalysis in the Povarov reaction and the basis for the high levels of stereoselectivity induced by **1a**. Similar enantioselectivities were achieved with a variety of sulfonic acids under homogeneous conditions, and we selected the **1a**/HOTf co-catalyzed reaction between **2a** and **3** as a model for mechanistic analysis. The reaction between **2a** (0.2–0.8 M) and **3** (0.4–1.6 M) promoted by catalytic quantities of CF_3SO_3H (HOTf, 0.2–2.0 mM) alone in toluene was monitored by reaction calorimetry and ^{1}H NMR spectroscopy (Table S4). Kinetic analysis of reactions carried out at 26 °C revealed a first-order dependence on [**3**] and [HOTf], and a zeroth-order dependence on imine [**2a**] (eq. 1). These data indicate that imine **2a** undergoes quantitative protonation by HOTf under the reaction conditions, and that protio-iminium triflate **2a•HOTf** represents the resting state of the achiral acid catalyst under the reaction conditions.

$$\text{Rate}=d[\mathbf{4}]/dt=k_{rac}[\text{imine}]_i^{0}[\mathbf{3}]_i^{1}[\text{HOTf}]_{tot}^{1} \quad (1)$$

Consistent with this conclusion, the reaction of imine **2a** with 1 equiv HOTf resulted in quantitative formation of protio-iminium triflate **2a•HOTf** as a moisture-sensitive salt that is sparingly soluble in non-polar solvents (ca. 2.0 mM in C_6D_6). The solubility of **2a•HOTf** increases by a factor of 4 in the presence of achiral urea **12** through the formation of the 1:1 complex (Fig. 3A). ^{1}H NMR chemical shifts of the formyl proton are sensitive probes of charge separation in iminium ions; (26) we observed that the 1:1 complex of **2a•HOTf** with achiral urea **12** exhibits a 0.14 ppm upfield shift of the ^{1}H NMR resonance of the formyl proton of **2a•HOTf**, consistent with increased charge separation. These observations can be attributed to a hydrogen bonding interaction between **12** and the triflate anion of **2a•HOTf** that leads both to solubilization and to greater charge separation between iminium ion and triflate anion.

Markedly different effects are observed when **2a•HOTf** is treated with solutions of bifunctional sulfinamidourea **1a**, which increases the solubility of **2a•HOTf** by more than one order of magnitude; however, dissolution is accompanied by a 0.92 ppm *downfield* shift of the ^{1}H-NMR resonance of the formyl proton of **2a•HOTf**, consistent with a less charge-separated iminium ion. Computational analysis (27) of the ternary **2a•HOTf•1a** complex suggests the basis for the observed effect. Four energetic minima were identified of comparable stability (Fig. 3B), with the **1a**-triflate complex acting as a dual H-bond acceptor through the triflate and sulfinamide groups, and the iminium ion as a dual H-bond donor through the iminium nitrogen and formyl protons (28).

The additional stabilizing interactions involving the catalyst-sulfinamide group and iminium ion formyl proton group have a pronounced effect on the rate of the Povarov reaction. Kinetic analysis of the reaction between **2a** and **3** co-catalyzed by HOTf and chiral sulfinamidourea **1a** under homogeneous conditions revealed that **1a** induces a substantial decrease in reaction rate (Fig. 3C). In contrast, the simple, achiral urea **12** has a slight accelerating effect (Fig. 3E). In the presence of **1a**, the reaction rate can be expressed by a two-term rate law in which the pathway catalyzed by HOTf alone dominates at low [**1a**], and a HOTf/**1a** co-catalyzed pathway dominates at high [**1a**] (eq 2). A binding constant of $K = 9000 \pm 2000\ M^{-1}$ for the interaction between **1a** and **2a•HOTf** can be determined from the kinetic data (Figures 3D, S11). This relatively high value stands in sharp contrast to the much weaker binding between chiral hydrogen bond donors and neutral substrates (29,30), but is consistent with binding constants determined between tetraalkylammonium salts and ureas and thioureas (31,32).

$$\text{Rate} = k_{\text{rac}}[\text{imine} \cdot \text{HOTf}] + k_{\text{asymm}}[\text{imine} \cdot \text{HOTf} \cdot \mathbf{1a}] \quad (2)$$

The observation of tight binding between protio-iminium triflate **2a•HOTf** and sulfinamido urea **1a** serves to explain how high enantioselectivity is obtained in the formation of **4a**, even under conditions where the HOTf-catalyzed racemic pathway is several times more rapid than the enantioselective pathway (Figures 3C–D): the equilibrium constant for complex formation is sufficiently high that virtually no free iminium ion exists, and the reaction is thus channeled through the asymmetric pathway. The enantioselectivity in the formation of $\mathbf{4a_{exo}}$ is increased further to synthetically useful levels by carrying out the reaction at lower temperatures (i.e. −55 °C, 97% ee).

In order to glean insight into the basis for stereoinduction in the Povarov reaction by sulfinamidourea catalyst **1a**, we carried out a full experimental and computational analysis of the mechanism of addition of dihydrofuran **3** to the protioiminium sulfate **2•HOTf•1a**. In principle, any of several elementary steps in this process may represent the rate- and

enantioselectivity-determining event (Fig. 4A, steps a–d). The absence of a primary kinetic isotope effect on the *ortho* hydrogens of the aniline group of **2** indicates that rearomatization (step d) is kinetically rapid (Fig 4B). A positive Hammett correlation was obtained in the analysis of the effect of anilino substituents on the rate of reaction ($\rho = +1.96 \pm 0.06$, Fig. S17). This result indicates that either the first step of a stepwise process (step a) or a concerted cycloaddition (step c) may be rate-limiting, but is inconsistent with the cyclization step of a stepwise process (step b) representing the slow step. Definitive distinction between steps a and c is more challenging (33), but the kinetic isotope effect data suggest that partial re-hybridization of the *ortho*-carbon of the aniline occurs in the rate-limiting step (34), and this is indicative of a concerted, albeit highly asynchronous [4+2] cycloaddition. This conclusion was supported by a computational analysis of the reaction leading to $\mathbf{4_{exo}}$, which predicts that the lowest energy pathway involves an endothermic cycloaddition, and a comparatively rapid deprotonation/rearomatization step (Fig. S19).

The catalyst-bound iminium ions depicted in Fig. 3B each have one π-face exposed to solvent and the other π-face shielded by the catalyst, and are all expected to be energetically accessible under the reaction condtions. Computational analyses using either density functional theory or ab initio methods (Fig. 4C–E) each predict that the enantioselectivity-determining cycloaddition occurs preferentially with complex **I**, leading to the experimentally observed (*R*)-enantiomer of product $\mathbf{4a_{exo}}$. The lowest energy cycloaddition transition structure displays iminium *N*-H···$O_{sulfinamide}$ and formyl C-H···$O_{sulfonate}$ hydrogen bonds (Fig. 4C), and is predicted to have ≥1.3 kcal/mol lower energy than alternatives arising from complexes **II**–**IV**, consistent with the experimental data. The basis for enantioselectivity may be ascribed to a stabilizing π-π interaction between the $(CF_3)_2$-C_6H_3N component of the catalyst and the cationic aniline moiety of the substrate. This interaction is evident in transition structures leading to the major enantiomer of $\mathbf{4a_{exo}}$ (Fig. 4D), but absent in transition structures leading the minor enantiomer (Fig. 4E).

Enantioselective catalysis by **1a** of a strong Brønsted acid-catalyzed Povarov reaction thus involves tight binding to a highly reactive cationic intermediate through multiple, specific H-bonding interactions, and these non-covalent interactions are maintained in the subsequent stereodetermining cycloaddition event. Remarkably, one of the four energetically accessible ground state complexes undergoes reaction with the nucleophile preferentially, illustrating the ability of bifunctional catalyst **1a** to precisely control the outcome of this reaction through non-covalent interactions alone. Given the known ability of urea and thiourea derivatives to bind a wide range of anions, the strategy demonstrated here is applicable, in principle, to cationic intermediates with a variety of counterion structures. (35)

Supplementary Material

Refer to Web version on PubMed Central for supplementary material.

Literature Cited

1. Eigen M. Angew Chem Int Ed 1964;3:1.
2. Akiyama T, Itoh J, Yokota K, Fuchibe K. Angew Chem Int Ed 2004;43:1566.
3. Uraguchi D, Sorimachi K, Terada M. J Am Chem Soc 2004;126:11804. [PubMed: 15382910]
4. Akiyama T. Chem Rev 2007;107:5744. [PubMed: 17983247]
5. Nakashima D, Yamamoto H. J Am Chem Soc 2006;128:9626. [PubMed: 16866505]
6. Hatano M, Maki T, Moriyama K, Arinobe M, Ishihara K. J Am Chem Soc 2008;130:16858. [PubMed: 19053478]
7. Ishihara K, Kaneeda M, Yamamoto H. J Am Chem Soc 1994;116:11179.

8. Yamamoto H, Futatsugi K. Angew Chem Int Ed 2005;44:1924.
9. Weil T, Kotke M, Kleiner CM, Schreiner PR. Org Lett 2008;10:1513. [PubMed: 18366220]
10. Klausen RS, Jacobsen EN. Org Lett 2009;11:887. [PubMed: 19178157]
11. Seebach D, Oei HA. Angew Chem Int Ed 1975;14:634.
12. Raheem IT, Thiara PS, Peterson EA, Jacobsen EN. J Am Chem Soc 2007;129:13404. [PubMed: 17941641]
13. Zhang Z, Schreiner PR. Chem Soc Rev 2009;38:1187. [PubMed: 19421588]
14. Doyle AG, Jacobsen EN. Chem Rev 2007;107:5713. [PubMed: 18072808]
15. Kouznetsov VV. Tetrahedron 2009;65:2721.
16. Ishitani H, Kobayashi S. Tetrahedron Lett 1996;37:7357.
17. Akiyama T, Morita H, Fuchibe K. J Am Chem Soc 2006;128:13070. [PubMed: 17017784]
18. Liu H, Dagousset G, Masson G, Retailleau P, Zhu JP. J Am Chem Soc 2009;131:4598. [PubMed: 19334771]
19. Materials and methods are detailed in Supporting Online Material available at *Science* Online
20. Tan KL, Jacobsen EN. Angew Chem Int Ed 2007;46:1315.
21. Leeson PD, et al. J Med Chem 1992;35:1954. [PubMed: 1534584]
22. Batey RA, et al. Chem Commun 1999:651.
23. Takamura M, Funabashi K, Kanai M, Shibasaki M. J Am Chem Soc 2001;123:6801. [PubMed: 11448184]
24. Witherup KM, et al. J Am Chem Soc 1995;117:6682.
25. Xia CF, Heng LS, Ma DW. Tetrahedron Lett 2002;43:9405.
26. Mayr H, Ofial AR, Wurthwein EU, Aust NC. J Am Chem Soc 1997;119:12727.
27. Frisch, MJ., et al. Gaussian 03, Revision E.01. Gaussian, Inc; Wallingford, CT: 2004.
28. Elia GR, et al. Can J Chem 1996;74:591.
29. Vachal P, Jacobsen EN. J Am Chem Soc 2002;124:10012. [PubMed: 12188665]
30. Schreiner PR, Wittkopp A. Org Lett 2002;4:217. [PubMed: 11796054]
31. Sessler, JL.; Gale, PA.; Cho, W-S. Anion Receptor Chemistry. RSC Publishing; Cambridge, U.K: 2006.
32. Kelly TR, Kim MH. J Am Chem Soc 1994;116:7072.
33. González J, Houk KN. J Org Chem 1992;57:3031.
34. Isaacs, N. Physical Organic Chemistry. John Wiley & Sons; New York: 1995. p. 296-301.

35. This work was supported by the NIH (GM-43214 and P50 GM-69721), and by fellowship support from the Dreyfus Foundation (to H.X.), the American Chemical Society and Roche (to S.J.Z.), and the American Chemical Society through the Irving S. Sigal Postdoctoral Fellowship (to M.G.W.). We thank Dr. Lars P. C. Nielsen for helpful discussions. Metrical parameters for a derivative of compound **4b$_{exo}$** are available free of charge from the Cambridge Crystallographic Data Centre.

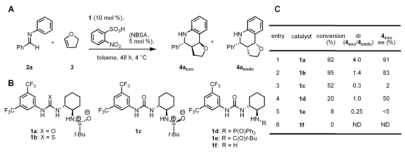

Figure 1.

(**A**) Model Povarov reaction co-catalyzed by *o*-nitrobenzenesulfonic acid and chiral ureas/thioureas. (**B**) Some of the chiral catalysts evaluated in optimization studies. (**C**) Results of catalyst structure-reactivity/enantioselectivity studies. d r = diastereomeric ratio. ee = enantiomeric excess. Both dr and ee were determined by supercritical fluid chromatography (SFC) analysis using commercially available chiral columns (Ref. 19).

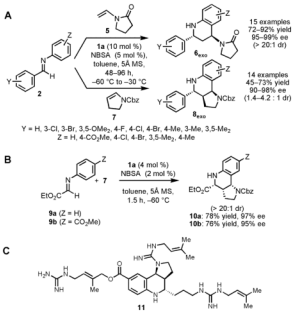

Figure 2.

(**A, B**) Asymmetric Povarov reactions catalyzed by **1a**/NBSA with enamide **5** and enecarbamate **7** as the nucleophilic reacting partners. Molecular sieves (5Å) serve to sequester water introduced with the hygroscopic NSBA reagent, thereby preventing competing imine hydrolysis pathways. See Tables S2–S3 for yields and selectivities obtained with each substrate. (**C**) Martinelline (**11**), a natural product inhibitor of bradykinin B1 and B2 G protein-coupled receptors (IC_{50} = 6.4 and 0.25μM, respectively). A previous study demonstrated that a racemic form of ester **10b** could be converted to (±)-**11** after epimerization of the corresponding aldehyde, so the enantioselective synthesis of **10b** described here constitutes a formal, enantioselective synthesis of martinelline (25).

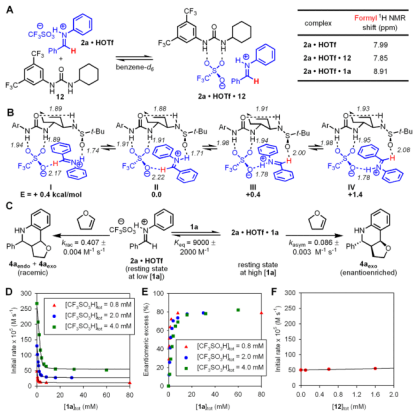

Figure 3.

(**A**) Formation of a complex between urea **12** and iminium sulfate **2•HOTf**. ^{1}H NMR chemical shifts of the formyl proton of **2a** as free and urea-bound salts. (**B**) Geometry and energy-minimized structures of **2a•HOTf•1a** calculated at the B3LYP/6-31G(d) level of density functional theory. Ar = 3,5-$(CF_3)_2C_6H_3$. (**C**) Kinetic parameters of racemic and enantioselective Povarov reaction of **2a** and **3** co-catalyzed by **1a** and HOTf. (**D**) Plot of initial rate of the Povarov reaction versus [**1a**] at three different concentrations of HOTf. [**2a**] = 0.4 M, [**3**] = 0.8 M. The black curves represent least-squares fits to the rate law derived from the kinetic scheme depicted in panel B. (**E**) Plot of ee of $\mathbf{4a_{exo}}$ versus [**1a**] at three different concentrations of HOTf. (**F**) Plot of initial rate of the racemic Povarov reaction co-catalyzed by achiral urea **12** and HOTf versus [**12**] with HOTf = 0.80 mM, [**2a**] = 0.4 M, [**3**] = 0.8 M.

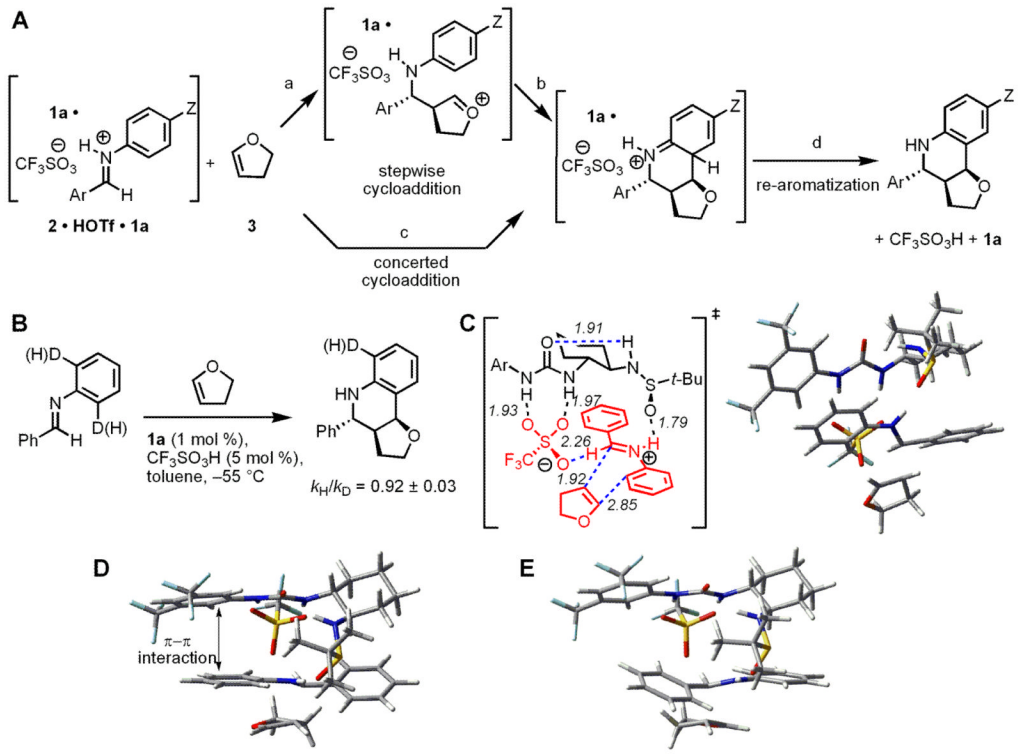

Figure 4.

(**A**) Possible mechanisms and rate-limiting steps in the asymmetric Povarov reaction. Z = an electron-donating or withdrawing substituent. (**B**) Kinetic isotope effect experiments to distinguish between different possible rate-limiting steps. (**C**) Geometry and energy-minimized lowest energy transition structure for cycloaddition calculated at the B3LYP/6-31G(d) level of density functional theory. Selected bond distances are shown in Å. Ar = 3,5-$(CF_3)_2C_6H_3$. (**D**) Alternate view of the structure in **C** highlighting the stabilizing π-π interaction between the aryl groups of the catalyst and the imimium ion undergoing cycloaddition. (**E**) Analogous view of the transition structure leading to the minor enantiomer of product. This transition structure lacks stabilizing π-π interactions, and is disfavored relative to the structure in D by 1.3 kcal/mol in calculations using the B3LYP/6-31G(d) method, and by 3.6–3.9 kcal/mol using M05-2X/6-31+G(d,p) or MP2/6-31G(d) single-point calculations. See Table S17 for further details.